

The structure of a cyanobiphenyl side chain liquid crystalline poly(silylenemethylene)

S.-Y. Park^a, T. Zhang^b, L.V. Interrante^b, B.L. Farmer^{c,*}

^aDepartment of Polymer Science, Kyungpook National University, Tsagu 702 701, South Korea

^bDepartment of Chemistry, Rensselaer Polytechnic Institute, Troy, NY 12180-3590, USA

^cAir Force Research Laboratory, Materials and Manufacturing Directorate, Wright-Patterson Air Force Base, OH 45433-7750, USA

Received 21 February 2002; accepted 26 February 2002

Abstract

The structure of a side chain liquid crystalline poly(silylenemethylene) $(-(\text{SiCH}_3\text{R}-\text{CH}_2)-; \text{R} = \text{O}(\text{CH}_2)_{11}\text{O}-\text{Ph}-\text{Ph}-\text{CN}, \text{Ph} = \text{phenyl})$ (CN-11) has been studied by X-ray diffraction and differential scanning calorimetry (DSC). The DSC results showed that CN-11 has transitions at $\sim 92^\circ\text{C}$ (T_2) and $\sim 147^\circ\text{C}$ (T_1) during both cooling and immediate heating. A third transition occurred at $\sim 50^\circ\text{C}$ (T_3) during heating after annealing at room temperature. The X-ray fiber pattern of the CN-11 annealed at room temperature showed several wide and small angle reflections which were indexed by a monoclinic unit cell with parameters $a = 16.8 \text{ \AA}$, $b = 7.42 \text{ \AA}$, $c = 43.6 \text{ \AA}$ and $\beta = 102.1^\circ$ (b : fiber direction), representing a crystal structure with layer thickness of $\sim 43 \text{ \AA}$. Upon heating at T_3 , the crystal structure became less ordered (but somewhat more ordered than smectic A (S_A) and smectic C (S_C)). This was followed by S_A (or S_C) phase at T_2 , and ultimately an isotropic state (I) at T_1 . The observed layer thickness ($\sim 43 \text{ \AA}$) is about ~ 1.5 times the most extended side chain length, indicating a double-layer structure with tilted or interdigitated side chains. The X-ray fiber pattern had a four-point pattern at $d = 4.52 \text{ \AA}$, suggesting that the side chains in the crystal are likely to be tilted by 56° from the polymer fiber axis. © 2002 Elsevier Science Ltd. All rights reserved.

Keywords: Poly(silylenemethylene); Hybrid polymers; X-ray diffraction

1. Introduction

Several poly(silylenemethylene)s, $[\text{SiRR}'\text{CH}_2]_n$, (PSMs) having a backbone of alternating Si and C atoms have been synthesized and characterized. [1–4] PSMs might be good candidates for side chain liquid crystal polymers because the Si–C backbone of these polymers is known to provide thermal stability similar to, or even better than, that of polysiloxanes [5]. Moreover, the Si–C backbone offers the prospect of improved backbone hydrolytic stability compared to polysiloxanes. Recently, PSM-based side chain liquid crystal polymers $(-(\text{SiCH}_3\text{R}-\text{CH}_2)-; \text{R} = \text{O}(\text{CH}_2)_N\text{O}-\text{Ph}-\text{Ph}, \text{Ph} = \text{phenyl})$ (PSM- N) were prepared and their structures were studied [6,8]. The PSM- N s showed well-ordered smectic phases having single-layer structures with an extended conformation in the alkyl spacer. These layered smectic structures persisted up to the isotropic temperatures during heating experiments. The kinds and number of smectic phases changed with spacer length. The mesogenic groups in the side chains of PSM-3 and PSM-6 packed in a two-dimensional orthorhombic cell,

characteristic of smectic E (S_E) phases. The mesogenic groups of PSM-8 and PSM-11 packed in a hexagonal smectic B (S_B) cell at room temperature. Crystalline structures developed during room temperature annealing of PSM-8 and PSM-11. Upon heating, the crystalline structures of PSM-8 and PSM-11 changed to smectic A (S_A) phases prior to becoming isotropic, whereas the S_E structure of PSM-3 changed directly into the isotropic state.

Another PSM-based side chain liquid crystal polymer $(-(\text{SiCH}_3\text{R}-\text{CH}_2)-; \text{R} = \text{O}(\text{CH}_2)_{11}\text{O}-\text{Ph}-\text{Ph}-\text{CN}, \text{Ph} = \text{phenyl})$ (CN-11) has been prepared [7]. CN-11 has the same chemical structure as PSM-11 except a cyano group is substituted at the end of the mesogen. Side chain liquid crystals containing polar CN substituents have been of special interest because the mesogens can be oriented in an electric field [9–11].

The structures of several side chain liquid crystalline polyacrylates and polymethacrylates with cyano-biphenyl substituents have been studied [11,12]. The polyacrylate $(-(\text{CHR}-\text{CH}_2)-; \text{R} = \text{OCO}(\text{CH}_2)_{11}\text{O}-\text{Ph}-\text{Ph}-\text{CN}, \text{Ph} = \text{phenyl})$ has a similar spacer length and the same mesogen as CN-11. It adopts a S_C structure at low temperature. This

* Corresponding author.

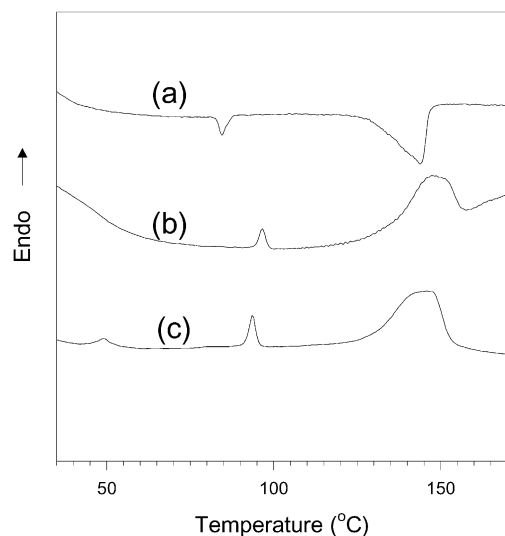


Fig. 1. DSC thermogram of CN-11 during (a) cooling, (b) immediate heating at 10 °C/min heating/cooling rate and (c) after annealing at room temperature for 1 day.

changes into a S_A phase at 30 °C and becomes isotropic at 145 °C. The polymethacrylate of $(-(CCH_3R-CH_2)-)$: $R = OCO(CH_2)_{11}O-Ph-Ph-CN$, $Ph = \text{phenyl}$) shows only a S_A structure and its isotropic temperature is 121 °C. Thus, the main chain of the polymer may influence the packing of mesogens in the side chain. In this paper, we report the highly ordered smectic structures of the CN-11. This polysilylenemethylene has a more flexible backbone than hydrocarbon backbone polymers.

2. Experiment

Fiber specimens for X-ray analysis were prepared by drawing (with tweezers) isotropic melts on a slide glass at ~ 90 °C. Wide-angle X-ray diffraction patterns were recorded on both Kodak Direct Exposure film and a phosphor image plate (Molecular Dynamics[®]) in a Statton camera. A Rigaku rotating anode X-ray generator, operated at 40 KV and 240 mA, produced Cu $K\alpha$ radiation, which was then monochromated. The sample to film distance was calibrated by SiO_2 powders. X-ray patterns at high temperatures were obtained using the heating accessory of the Statton camera.

DSC experiments were carried out in a Perkin–Elmer DSC-7. The temperature and heat flow scales were calibrated using standard materials. The sample size was ~ 1.5 mg. For cooling scans, the samples were heated above their isotropic temperatures for 2 min and then cooled to 20 °C at controlled cooling rates ranging from -10 to -40 °C/min. For heating scans, the samples were first cooled from 170 (isotropic state) to 20 °C at a rate of -10 °C/min. They were then heated at different heating rates ranging from 10 to 40 °C/min. The transition tempera-

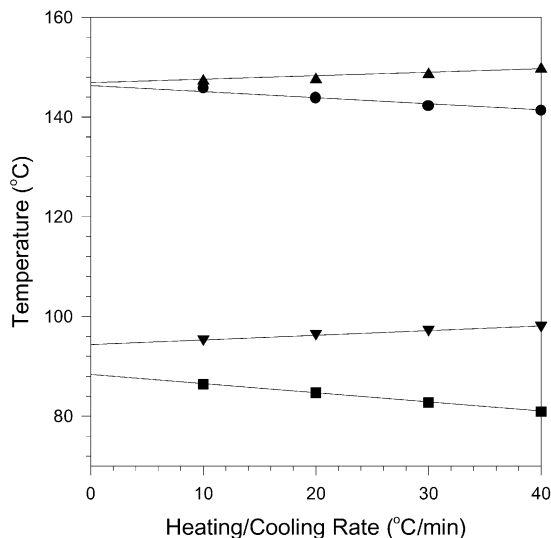


Fig. 2. T_{h1} , T_{h2} , T_{c1} and T_{c2} of CN-11 at 10–40 °C/min: (▲) T_{h1} , (▼) T_{h2} , (●) T_{c1} , (■) T_{c2} (the lines are least-square fits to the data).

tures were determined from the maximum points of the transition curves.

3. Results and discussion

3.1. Phase transition

Fig. 1(a) and (b) show DSC thermograms of CN-11 during cooling and immediate heating. CN-11 showed transitions at 95 °C (T_{h2}) and 146 °C (T_{h1}) during heating (curve b) and at 85 °C (T_{c2}) and 144 °C (T_{c1}) during cooling (curve a). The enthalpy at T_{h2} and T_{c2} (~ 0.6 J/g) was much less than that at T_{h1} and T_{c1} (~ 5.9 J/g), suggesting that only minor structural change occurred through the transition at T_2 . The isotropic transition, T_1 , was confirmed through the polarizing optical microscopy.

Fig. 2 plots T_{h1} , T_{h2} , T_{c1} and T_{c2} of the CN-11 at heating/cooling rates from 10 to 40 °C/min. The transition temperatures depend on the heating/cooling rates. The degree of supercooling (ΔT), i.e. the difference of transition temperatures measured in the heating and cooling experiments, decreases as the heating/cooling rates decrease. Equilibrium transition temperatures (T°) can be determined by extrapolating to zero cooling/heating rate: T_{h1}° and T_{c1}° are 147 °C and the degree of supercooling at zero cooling/heating rate, (ΔT_1°), is ~ 0 °C. T_{h2}° is 94 °C and T_{c2}° is 90 °C and the degree of supercooling at zero cooling/heating rate, (ΔT_2°), is ~ 4 °C. One of the characteristics of liquid crystalline materials is that the degree of supercooling of a liquid crystal is much smaller than that of crystalline material, and that of a high order liquid crystal phase is larger than that of a low order liquid crystal phase. The value of ΔT_1° , 0 °C, clearly indicates that the transition at T_1 is related to a low order liquid crystal structure. However, the value of ΔT_2° ,

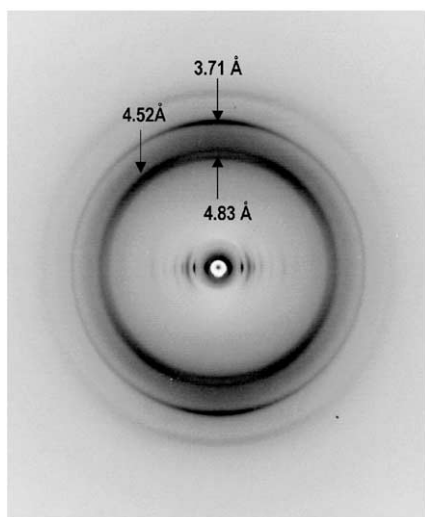


Fig. 3. The X-ray fiber pattern of the CN-11 after annealing at room temperature for 1 day.

~ 4 °C, suggests that the transition at T_2 is related to a somewhat higher order structure. This is consistent with X-ray data, which show a high order structure (higher than S_A and S_C) below T_2 (discussed later).

Fig. 1(c) shows the DSC thermogram of a sample annealed at room temperature for 1 day. A new transition was observed at ~ 50 °C (T_{3h}). The appearance of a new transition after room temperature annealing for long times is often observed for side chain liquid crystal polymers. The transitions are attributed to melting of crystalline order formed during annealing [8,13]. The rate of crystallization of CN-11 was apparently too slow for the transition to appear in samples heated immediately after the cooling experiment. In order to study the structure of CN-11 and the changes which occur during the thermal transitions, X-ray diffraction was employed.

3.2. X-ray fiber patterns

Fig. 3 shows the X-ray fiber pattern of CN-11 after annealing at room temperature for 1 day. There is a series of sharp reflections at $d = 42.6, 21.3, 14.2$ Å (orders of 42.6 Å) and several other reflections at $d = 16.5, 11.8, 9.7$ and 7.81 Å along the equator. There are also several reflections at $d = 4.83, 3.71$ and 3.21 Å in the wide-angle region, which are stronger along the meridian than along the equator. The reflection at $d = 4.52$ Å has a maximum 34° from meridian in the azimuthal direction (discussed later). The several sharp equatorial and wide-angle reflections strongly suggest that the drawn fiber annealed at room temperature has a crystalline structure (or highly ordered smectic phase), not just liquid crystalline ordering. All equatorial reflections can be indexed on the basis of a two-dimensional monoclinic lattice with reciprocal cell dimensions of $a^* = 1/16.45$ (Å $^{-1}$), $c^* = 1/42.6$ (Å $^{-1}$) and $\beta^* = 77.9^\circ$. (The b dimension is along the fiber direction. This is keeping with common

Table 1

The observed and calculated d -spacings for CN-11. Unit cell parameters were $a = 16.8$ Å, $b = 7.42$ Å, $c = 43.6$ Å and $\beta = 102.1^\circ$

H	k	l	$d_o(\text{Å})$	$d_c(\text{Å})$
0	0	1	42.7	42.6
0	0	2	21.3	21.3
1	0	0	16.5	16.5
0	0	3	14.2	14.2
1	0	2	11.9	11.9
1	0	3	9.65	9.78
2	0	1	7.80	7.78
0	1	0	7.42	7.42
2	1	3	4.83	4.91
-3	1	2	4.52	4.47
-3	1	1		4.46
3	1	2	4.18	4.18
0	2	0	3.71	3.71
-2	2	1	3.38	3.39
2	2	3	3.21	3.23

practice for liquid crystal materials. Since the polymer backbone does not contribute significantly to the diffraction pattern, the c direction is defined with respect to the liquid crystal side chains rather along the fiber direction.) The sharp equatorial reflections at $d = 42.7, 21.3, 14.2$ Å can be indexed as 001, 002 and 003, respectively and the reflections at $d = 16.5, 11.9, 9.65$ and 7.80 Å can be indexed as 100, 102, 103 and 201 as shown in Table 1. Note that these two groups of reflections have different characters. The orders of the layer spacing are significantly sharper. The calculated d -spacings are in good agreement with the observed values.

In addition to the strong reflection at $d = 3.71$ Å, there is a very weak reflection at $d = 7.42$ Å on the meridian (It is so weak that it can be observed only by close examination and controlling contrast in the digital image.) The indices for these reflections are 020 and 010, respectively. If the crystal structure is monoclinic (where b is the unique axis), the b^* parameter would be $1/7.42$ (Å $^{-1}$). The real space lattice parameters are therefore $a = 16.8$ Å, $b = 7.42$ Å, $c = 43.6$ Å and $\beta = 102.1^\circ$ for the crystalline form of CN-11. This unit cell is similar to a smectic structure having monoclinic symmetry which is denoted as smectic G (S_G) and first observed in side chain liquid crystalline polymers by Shibaev et al. in 1986 [13,14]. The X-ray fiber pattern is also very similar to that reported by Atkins et al. [15,16]. They defined it as a crystalline structure. Similarly, we define this structure as a crystalline structure having monoclinic symmetry.

The layer thickness of CN-11 is 43.6 Å (c dimension; 42.7 Å is for c^*) and the planes of the layers are parallel to the fiber axis. We reported earlier the smectic structure of PSM-11, which has the same chemical structure as CN-11 but without the cyano group in the mesogen. PSM-11 has a single-layer structure with layer thickness of 29.1 Å, corresponding to the most extended length of the side chain. The layer thickness of CN-11 is much larger than that of

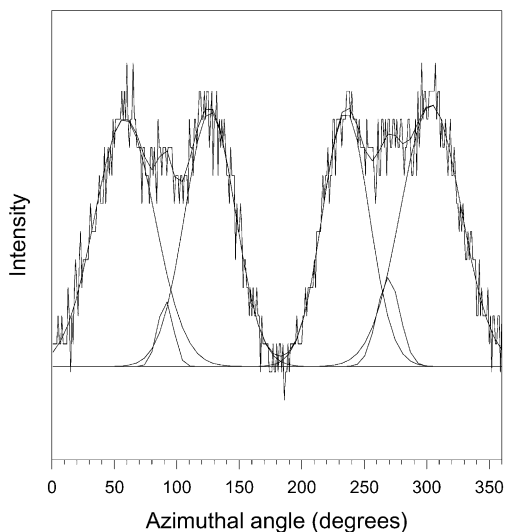


Fig. 4. The azimuthal scan of Fig. 3 at $d = 4.52 \text{ \AA}$ (0°) along the equatorial direction and solid lines are curve-fits to the data.

PSM-11, indicating that CN-11 has a double-layer structure. However, the layer thickness of the CN-11 is much less than twice the most extended chain length ($\sim 56 \text{ \AA}$). Thus, the side chains are either partially interdigitated or tilted within the smectic layers from the direction normal to the main chain (and fiber) axis. The strong reflection at $d = 4.52 \text{ \AA}$ is split into four reflections. Fig. 4 shows the azimuthal scan at $d = 4.52 \text{ \AA}$. The small maxima at 90 and 270° (meridional directions) are part of the meridional reflection at $d = 3.71 \text{ \AA}$. The four reflections are separated from the meridian by 34° in the azimuthal direction. Side chain liquid crystalline polymers having similar mesogenic groups usually have a reflection at $d = 4.4 \pm 0.1 \text{ \AA}$ representing the distance between the hexagonally packed mesogens [11]. This four-point pattern here strongly suggests that the side chains are tilted by 56° from polymer fiber axis. Such a tilted side chain structure is observed in the smectic C (S_C) structure of the polyacrylate having the same mesogen as CN-11 and a similar side chain length [11,12].

3.3. Structural transitions

Fig. 5 shows X-ray fiber patterns at different temperatures. The observed d -spacings are listed in Table 2. The room temperature pattern (Fig. 5(a)) does not change at 35°C . At 45°C (close to T_{h3} in the DSC thermogram (Fig. 1(c))), some wide-angle reflections weaken and an amorphous halo appears in the meridional direction (Fig. 5(b)). A weak reflection at $d = 4.52 \text{ \AA}$ (arrow in Fig. 5(b)) remains. The equatorial reflections at $d = 42.7$ (001) and 21.3 \AA (002) are unchanged. The equatorial reflection at $d = 16.5 \text{ \AA}$ (100) becomes diffuse and shifts slightly to $d = \sim 15 \text{ \AA}$. The reflection at $d = 11.9$ (102) (arrow in Fig. 5(b)) remains sharp but shifts slightly to 12.0 \AA . The existence of the 102 reflection suggests that the mono-

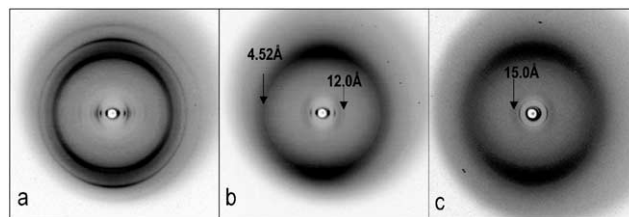


Fig. 5. The X-ray fiber patterns at (a) $25\text{--}35^\circ\text{C}$, (b) $45\text{--}95^\circ\text{C}$ and (c) $105\text{--}125^\circ\text{C}$.

clinic symmetry may remain even though much of the order in the crystal structure was lost at T_{h3} , evident from the disappearance of all wide-angle reflections except for the reflection at $d = \sim 4.5 \text{ \AA}$. (It is difficult to determine whether the four-point pattern at $d = \sim 4.5 \text{ \AA}$ remains because the reflection becomes so broad in the azimuthal direction.) The X-ray fiber pattern becomes similar to that of S_A (or S_C) except for two sharp reflections at $d = \sim 4.5$ and 12.0 \AA . A S_A pattern has only ordered equatorial reflections and a broad meridional reflection in the X-ray fiber pattern. A S_C pattern has only ordered equatorial reflections and broad, split wide-angle reflections. It is unclear whether the reflection at $d = \sim 4.5 \text{ \AA}$ is split or not. However, it is obvious that there is a lot of statistical disorder giving the broad reflections. These two remaining reflections suggest that the material has higher order than S_A and S_C but less than the crystal structure at room temperature.

The X-ray fiber pattern changed little between 45 and 95°C . Fig. 5(c) shows the fiber pattern at 105°C , close to T_{h2} in the DSC thermogram. The weak reflection at $d = 4.5 \text{ \AA}$ is gone and there is only an amorphous halo in the wide-angle region. The equatorial reflection at $d = 12.0 \text{ \AA}$ has also disappeared. Fig. 5(c) is typical of a S_A (or S_C) pattern except for the diffuse scattering at $d = \sim 15 \text{ \AA}$ (arrow in Fig. 5(c)). The latter may be due to the stacking disorder of the smectic sheets in the direction perpendicular to the side chains. This kind of ordering is similar to a cybotactic structure, which often exhibits a diffuse small angle reflection [17,18].

Fig. 6 shows the d -spacings of the first equatorial reflection at different temperatures. The d -spacing decreases from ~ 42 to $\sim 38 \text{ \AA}$ at $\sim T_2$ ($\sim 95^\circ\text{C}$). Below T_2 , the crystal structure has tilted side chains. Above T_2 , the S_A (or S_C) structure was observed. The decrease observed in the layer thickness strongly suggests that the spacers may have melted into an amorphous phase. The wide-angle reflection is so broad in the 2θ and azimuthal directions that it is difficult to detect significant side chain ordering in the wide-angle region. However, two sharp equatorial small angle reflections persist up to the isotropic temperature and suggest that the smectic structure is not destroyed before that. This may be due to the strong interactions between mesogenic groups having polar CN groups.

Table 2
The observed d -spacings (Å) of CN-11 at different temperatures

25 °C	35 °C	45 °C	55 °C	65 °C	75 °C	85 °C	95 °C	105 °C	115 °C	125 °C
42.7	43.1	42.6	42.7	42.4	42.0	39.2	38.4	37.6	36.8	34.7
21.3	21.3	21.2	21.3	20.6	20.5	19.9	19.5	19.4	18.9	18.3
16.5	16.5	~ 15	~ 15	~ 15	~ 15	~ 15	~ 15	~ 15	~ 15	~ 15
14.2	14.2									
11.9	11.9	12.0	12.0	12.1	12.1	12.1	12.1			
9.65	9.65									
7.80	7.80									
4.83	4.83									
4.52	4.52	4.51	4.51	4.55	4.54	4.54	4.54			
4.18	4.18									
3.71	3.71									
3.38	3.38									
3.21	3.21									

4. Conclusions

The structure of a side chain liquid crystalline poly(silylenemethylene) $-(\text{SiCH}_3\text{R}-\text{CH}_2)-$; $\text{R} = \text{O}(\text{CH}_2)_{11}\text{O}-\text{Ph}-\text{Ph}-\text{CN}$, $\text{Ph} = \text{phenyl}$ (CN-11) has been studied by X-ray diffraction and DSC. DSC results show that CN-11 has structural transitions at $\sim 95^\circ\text{C}$ (T_2) and $\sim 146^\circ\text{C}$ (T_1) during both cooling and immediate heating. A third transition was observed at $\sim 50^\circ\text{C}$ (T_3) during heating after the sample had been annealed at room temperature. The X-ray fiber pattern of CN-11 annealed at room temperature shows several wide and small angle reflections which can be indexed by a monoclinic unit cell with parameters of $a = 16.8 \text{ \AA}$, $b = 7.42 \text{ \AA}$, $c = 43.6 \text{ \AA}$ and $\beta = 102.1^\circ$ (b : fiber direction), suggesting that the structure below T_3 is a crystal structure. On heating at T_3 , the crystal structure became less ordered. This is followed by a smectic A (or C) phase at T_2 , and ultimately an isotropic state (I) at T_1 . The

observed layer thickness ($\sim 42 \text{ \AA}$) is about 1.5 times the extended chain length for one side chain, indicating a double-layer structure with either tilted or the interdigitated side chains. The four-point character of the reflection at $d = 4.52 \text{ \AA}$ strongly suggests that the side chains in the layers are tilted.

Acknowledgements

Support from the National Science Foundation through grant DMR-9731345 is gratefully acknowledged. S.-Y. Park also acknowledges support from the Air Force Office of Scientific Research for an NRC post-doctoral research associateship.

References

- [1] Rushkin I, Interrante LV. *Macromolecules* 1996;29:3123.
- [2] Interrante LV, Liu Q, Rushkin I, Shen Q. *J Organomet Chem* 1996;521:1.
- [3] Rushkin I, Interrante LV. *Macromolecules* 1996;29:5784.
- [4] Tsao MW, Rabolt J, Farmer BL, Interrante LV, Shin Q. *Macromolecules* 1996;29:7130.
- [5] Levin G, Carmichael JB. *J Polym Sci A-1* 1968;6:1.
- [6] Zhang T, Park SY, Farmer BL, Interrante LV. *ACS Polym Prepr* 2000;41(1):975.
- [7] Zhang T, Park SY, Farmer BL, Interrante LV. *ACS Polym Prepr* 2002.
- [8] Park SY, Zhang T, Interrante LV, Farmer BL. *Macromolecules* 2002;35:2776.
- [9] Finkelmann H, Naegele D, Rindgsdorf H. *Macromol Chem* 1979;180:803.
- [10] Tal'rose RV, Kostromin SG, Shibaev VP, Plate NA, Kresse H, Zauer K, Demus D. *Makromol Chem Rapid Commun* 1981;2:305.
- [11] Kostromin SG, Sinitsyn VV, Tal'rose RV, Shibayev VP. *Polym Sci USSR* 1984;26(2):370.
- [12] Plate NA, Tal'rose RV, Freidzon YS, Shibaev VP. *Polym J* 1987;19(1):135.
- [13] Freidzon YS, Boiko NI, Shibaev VP, Tsukruk VV, Shilov VV, Lipatov YS. *Polym Commun* 1986;27:190.

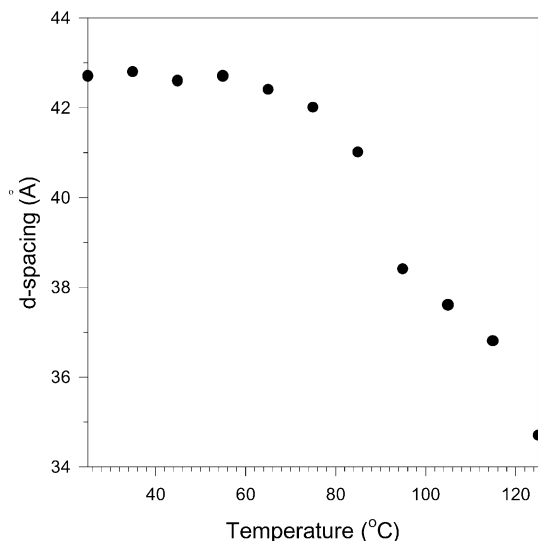


Fig. 6. d -Spacings of the first equatorial reflection.

- [14] Platè NA. Liquid-crystal polymers. New York: Plenum Press, 1993. Chapter 6; p. 222.
- [15] Singler RE, Willingham RA, Noel C, Friedrich C, Bosio L, Atkins EDT. *Macromolecules* 1991;24:510.
- [16] Jaglowski AJ, Singler RE, Atkins EDT. *Macromolecules* 1995;28:1668.
- [17] Duran R, Gramain P, Guillon D, Skoulios A. *Mol Cryst Liq Cryst Lett* 1986;3:23.
- [18] Duran R, Guillon D, Gramain P, Skoulios A. *Makromol Chem Rapid Commun* 1987;8:321.